

## Crossover between Spatially Confined Precipitation and Periodic Pattern Formation in Reaction Diffusion Systems

E. López Cabarcos,<sup>1,\*</sup> Chein-Shiu Kuo,<sup>2</sup> A. Scala,<sup>1</sup> and R. Bansil<sup>1</sup>

<sup>1</sup>Center for Polymer Studies, Department of Physics, Boston University, Boston, Massachusetts 02215

<sup>2</sup>Department of Chemistry, Boston University, Boston, Massachusetts 02215

(Received 19 June 1996)

We have observed a crossover between a spatially confined precipitation regime and periodic pattern formation regime. This unusual behavior was observed when electrolyte solutions of  $\text{Na}_2\text{HPO}_4$  and  $\text{CaCl}_2$  were allowed to diffuse into an agarose gel from opposite ends. The formation of the confined precipitate occurs when the electrolyte flux  $J$  is the same at both sides of the gel. The time of formation and the width of the precipitate are a function of  $J$  and both follow the scaling relation  $\omega \sim (J/D)^{-\beta}$  with  $\beta = 0.40 \pm 0.2$  and  $D$  the diffusion coefficient. The growth of periodic bands of precipitate was observed when  $J$  was different at both gel ends. [S0031-9007(96)01256-2]

PACS numbers: 82.20.-w, 05.40.+j, 05.50.+q, 81.10.Aj

There has been much recent interest in the properties of the one dimension reaction front in  $A + B \rightarrow C$  (solid) diffusion reaction systems [1–5]. Particular attention has been paid to systems where the initially separated reactants after diffusing are allowed to react irreversibly and the products  $C$  are inert particles which may diffuse [6] or not [7]. Among the reaction diffusion controlled systems one of the most interesting cases occurs when an electrolyte front diffuses and reacts with another electrolyte which is embedded in a gel. The chemical reactions between the salts lead to a slightly soluble product that precipitates discontinuously in bands parallel to the diffusion front's surface. This phenomenon, called Liesegang bands, has been widely studied because it offers a model to explain a great variety of formations in nature, ranging from agate rocks and gold veins to the growth of bacterial rings in agar and gallstones [8–15]. The patterns appear to follow some general laws. First, the position  $x_n$  (measured from the gel surface) of the  $n$ th band is related to the time  $t_n$  of its formation by the so called time law  $x_n \sim t_n^{1/2}$  which is the hallmark of the diffusion mechanism. Second, the ratio between the positions of adjacent bands,  $x_n/x_{n-1} = p$ , approaches a constant value  $p > 1$  for large  $n$  although the phenomenon of reverse banding, i.e.,  $p < 1$  has sometimes been observed. Third, the width of the bands  $\omega_n$  grows with the distance according to the relation  $w_n \sim (x_n)^\alpha$  with  $\alpha$  smaller than 1.

Many theoretical and simulation studies have been made to explain the formation of Liesegang patterns. No single model can explain all the observed results, such as the presence of precipitate particles between the bands, the reverse spacing ( $p < 1$ ) phenomena, or the formation of complex patterns (double banding). However, there is considerable evidence to support the supersaturation theory of Ostwald and Prager which considers band formation as a spatially discontinuous nucleation process [6,7]. The formation of sharp rings is

preceded by the onset of a turbidity front, implying that colloidal particles are continuously distributed initially and the sharp band formation is a post nucleation process involving aggregation and growth mechanisms [16].

Recently there has been renewed interest in the study of periodic precipitations because the possibility of simulating the process allows more quantitative predictions. Mean-field models [17,18] and more recently cellular automata models [13,19] have been proposed to describe in a more accurate and quantitative manner the formation of periodic patterns. The related phenomenon of diffusion limited reactions, without pattern formation, has also been modeled quite extensively in recent years.

In the usual Liesegang experiment one electrolyte is present in the gel and the other one, typically at a much higher concentration, diffuses in from one boundary. The question of whether Liesegang bands will form if both reactants diffuse from opposite boundaries has, to the best of our knowledge, never been addressed. Such a system offers the possibility of (i) determining if a crossover between a continuous diffusion-reaction front and a discrete periodic precipitation regime can be obtained, and (ii) to examine if the scaling and mean-field theoretical predictions for the reaction-diffusion fronts are valid for the precipitate front.

In this Letter we report an experimental and numerical study of the formation of the precipitate in a system in which a flux  $J$  of  $A$  and  $B$  electrolyte particles are applied at the opposite boundaries of a gel. We have selected for our work agarose gel and two salts,  $\text{Na}_2\text{HPO}_4$  and  $\text{CaCl}_2$  as reagents because the low solubility of one of the reaction products ( $\text{CaHPO}_4$ ). We have followed the kinetics of formation of the precipitate in both cases and we have investigated the influence of the electrolyte flux on the dimensions of the precipitate. Concurrently, a simulation of the behavior of these systems, in terms of mean-field rate equations for the densities of  $A$ ,  $B$ , and  $C$  particles is presented.

Aqueous solutions of the two salts were allowed to diffuse into a 1.5% agarose gel of length 2 cm in a 2 mm diameter glass capillary. The time evolution of the precipitate was recorded using a charge-coupled device camera and the images were stored on a videotape and analyzed using a frame-grabber and digital image analysis program.

Figure 1 shows an image of the gel recorded 10 days after the initiation of the reaction. An intensity profile along the length of the gel is traced below the photograph. The ratio of the reactant concentrations appears to have a profound effect on the precipitation profile. A spatially confined precipitation front occurs for the equal concentrations (lower panel), whereas Liesegang bands appear when the concentrations at both ends of the gel are different (upper panel). Similar results were obtained over a wide range of concentrations. The profiles remain practically identical 5 months later, which seems to indicate that the precipitation was complete after the first couple of weeks.

In an attempt to reproduce the observed behavior we have performed numerical simulations with the diffusion-reaction model. We have assumed that in the reaction  $A + B \rightarrow C$ , the product  $C$  is a neutral molecule capable of diffusing and aggregating. The aggregation is modeled by an additional reaction  $C \rightarrow D$  where  $D$ , although chemically identical to  $C$ , represent the solid phase. The

reaction term is expressed in the mean-field form  $Kab$  of a two molecule irreversible collision process with a constant reaction rate. We have ignored the reverse process  $C \rightarrow A + B$ . This assumption relies on the experimental fact that we are dealing with ions that form weakly soluble species which leads to a simplification for these coupled partial differential equations with nonlinear terms.

Following Dee's [6] simplification we have considered that the aggregation term consists of two parts: the first one accounts for nucleation and has the form  $K_n c$  for  $c > c_n$ , where  $c_n$  is the supersaturation threshold at which nucleation is no more hindered by kinetic barriers. Nucleation is assumed to be the only mechanism responsible for the triggering of the precipitation in the gel because cluster-cluster aggregation is inhibited by the trapping of mesoscopic particles in the gel structure. The second part of the precipitation term is in general a complicated integro-differential expression [6,20] of the concentration of  $C$  and  $D$ . It is based on the fact that in the presence of aggregation, precipitation of nuclei is no more hindered by kinetic barriers and occurs for concentration  $c > c_s$ , where  $c_s$ , the saturation threshold is  $< c_n$ . In order to simplify the equations, we have followed the Chopard *et al.* approach [19] and have retained the nonlinear term  $K_p c d$  so that our simplified equations become

$$\begin{aligned}\delta_t a &= D_a \nabla^2 a - Kab, \\ \delta_t b &= D_b \nabla^2 b - Kab, \\ \delta_t c &= D_c \nabla^2 c + Kab - K_n c H(c - c_n) \\ &\quad - K_p c d H(c - c_s), \\ \delta_t d &= K_n c H(c - c_n) + K_p c d H(c - c_s),\end{aligned}\quad (1)$$

where  $H(x)$  is the Heaviside step function.

The results obtained by numerically integrating Eq. (1) are shown in the insets of Fig. 1. In the case of equal electrolyte concentrations we obtain a continuous precipitate similar to the experimental one. The formation of the Liesegang bands is simulated by just changing the initial electrolyte concentrations at both gel extremes and keeping the rest of the parameters unchanged.

Although the formation of Liesegang rings in gels is a well known phenomenon, the occurrence of a drastic change from a spatially confined precipitate to a regime of periodic precipitates to our knowledge has not yet been investigated. Chopard *et al.* performed simulations with cellular automata models [19] of the Liesegang rings and predicted different possible pattern formation as a function of the values of  $K_{nuc}$  and  $K_p$ . The only influence that these authors have attributed to the concentration gradient appears in the  $\alpha$  exponent of the expression that gives the bandwidth as a function of the precipitate position  $w_n \sim (x_n)^\alpha$ . They reported that the exponent  $\alpha$  decrease from 0.6 to 0.5 when decreasing the initial electrolyte concentration differences ( $a_0 - b_0$ ). No predictions

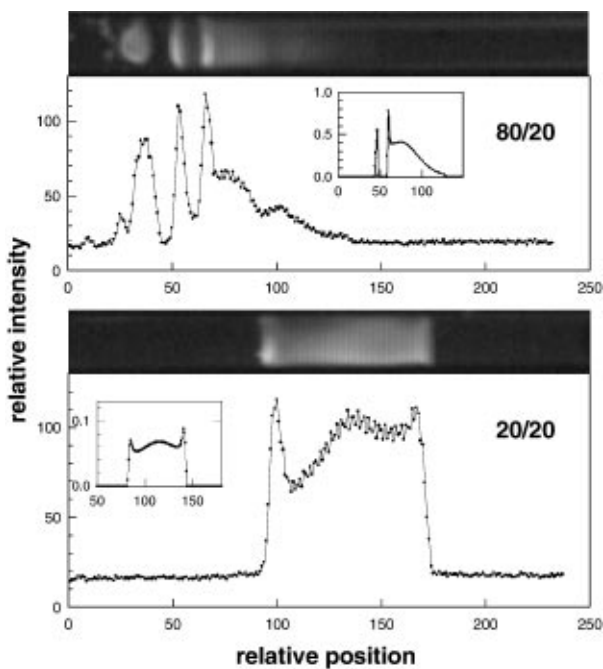


FIG. 1. Photograph showing the different precipitates in an agarose gel when  $\text{Na}_2\text{HPO}_4$  and  $\text{CaCl}_2$  diffuses from both ends of the gel. The electrolyte concentrations in mM are (a) 80/20 and (b) 20/20. Below the images we display the precipitation profiles. In the insets we show the simulated profiles calculated using Eq. (1) with  $K = 0.1$ ,  $K_n = 0.02$ ,  $K_p = 0.8$ ,  $D_a = 1.7$ ,  $D_b = 1.2$ ,  $D_c = 1.8$ ,  $c_n = 0.003$ , and  $c_s = 0.0005$ .

were made for equal electrolyte concentrations. Our investigations show that the precipitation profile may vary depending upon having equal electrolyte concentrations or not.

When the electrolyte concentrations on the two sides are equal, the flux  $J$  would be the same at both ends. As illustrated in Fig. 2 we found that with equal electrolyte concentrations ranging from 10 mM to 1 M the precipitation front becomes increasingly narrow as the concentration increases. In Fig. 3 we show the log-log dependence of the time of formation and width of the precipitate front versus the electrolyte concentration. The width follows a relation  $\omega \sim (J/D)^{-\beta}$ , with  $\beta = 0.40 \pm 0.02$ . The time at which the precipitate could be first detected by the imaging system also follows the same power-law dependence on the concentration.

The inhomogeneous mean-field description predicts a reaction front width which scales as  $\omega \sim (J/D^2)^{-1/3}$ . For  $d = 1$  it was proposed [5] that the fluctuations modify the scaling of the width to  $\omega \sim (J/D)^{-1/2}$ . The time of formation of the precipitate is predicted follow a relation of the type  $t_c = (\frac{1}{c})^{1/2}$

The profile of the reaction front was fitted better with the prediction of the mean-field model, than with the Gaussian form predicted by the fluctuation modified model for the high concentration case (80/80). The

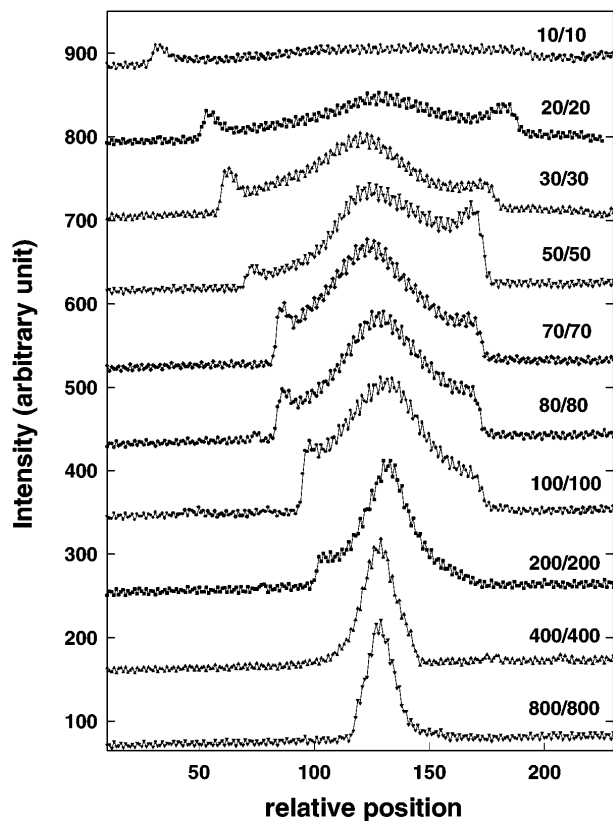


FIG. 2. Dependence of the precipitation profile with the electrolyte concentration.

reverse was observed for the low concentration case (20/20), implying that fluctuation effects are more pronounced at lower concentrations when the precipitation is slower than at higher concentrations when the precipitation occurs faster.

Even though the  $\beta$  value obtained is larger than the one predicted by the mean-field theory for the reaction front it suggests that the profile of the aggregation front approximates that of the reaction front. This means that the diffusion of the particles formed in the reaction front should be small. If we consider the precipitation profile as the addition of a reaction front in the center and two Liesegang bands at the borders then we can write, using the mean-field prediction,

$$\frac{\omega_{\text{center}}}{\omega_{\text{wings}}} = \left( \frac{D_{\text{center}}}{D_{\text{wings}}} \right)^{2/3} \quad (2)$$

We find that  $\omega_{\text{wings}} < \omega_{\text{center}}$ ; hence  $D_{\text{wings}}/D_{\text{center}} < 1$ , which implies that the average size of the particles should be larger at the lateral bands than in the center of the precipitate. This prediction agrees very well with the finding of Le Van and Ross [9] that the size of the particles inside a band increases towards the outermost border in the direction of the diffusion front. Inside the two bands that confined the precipitate the larger particles would grow through an Ostwald ripening mechanism constituting somewhat like the bricks of the walls that enclose the precipitate front.

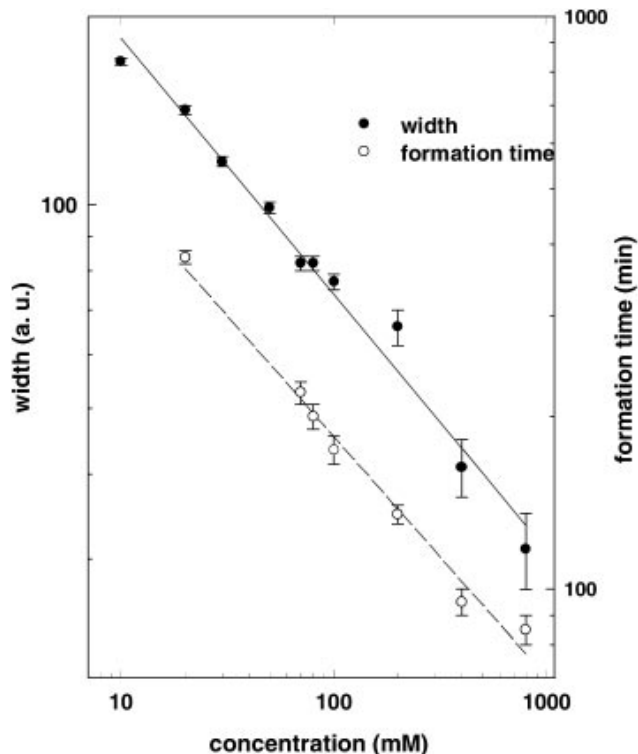


FIG. 3. Log-log plot of the time of formation and profile width versus the concentration.

In the case of unequal concentrations we obtained periodic precipitation. The position of the bands, measured from the center of the precipitate, follows a similar spacing law to the bands formed when the  $\text{CaCl}_2$  is embedded in the gel. Only the value of the spacing parameter  $p = 1.4$  seems somewhat larger than the  $p = 1.2$  found when the electrolyte is embedded in the gel. Furthermore, the time law is also fulfilled and there are not sufficient number of bands to check the predictions for the width law. One of the most striking features we have observed is the asymmetry at the early stages of the precipitation profile before the Liesegang bands were formed in contrast to the very symmetric profiles corresponding to the formation of the confined precipitate. Although the symmetry in the profile is a consequence of the symmetry in the flux, it looks as if only small differences in electrolyte concentration are required to achieve Liesegang bands.

Figure 4 shows the profiles obtained for the different electrolyte concentration ratios. In all cases bands developed, even though for the 10/20 and 25/20 more than 1 week would be required to observe the second band. This

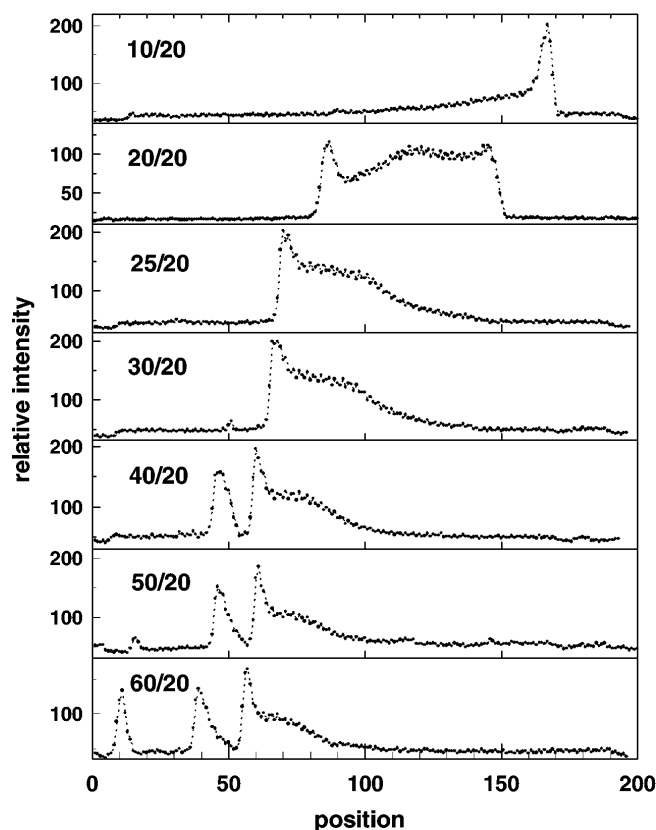


FIG. 4. Crossover between the spatially confined precipitate to the periodic Liesegang regime as a function of the concentration gradient. The patterns were recorded 1 week after the initiation of the experiment.

implies that under the conditions described above, only a small difference in electrolyte concentration is required to obtain periodic patterns.

Although the scaling behavior of the real system is not fully mimicked, we have been able to reproduce easily the patterns experimentally observed.

We have observed a crossover between a regime of spatially confined precipitate to a regime of periodic precipitation. We have demonstrated that the electrolyte flux is the main parameter defining the type of precipitate formed. Furthermore, for equal electrolyte fluxes we have found a scaling law for the width of the precipitate profile and its time of formation similar to that found in  $A + B \rightarrow C$  reaction-diffusion fronts.

E. Lopez Cabarcos acknowledges DGICYT and the Complutense University for granting support for a Sabbatical year and Professor H.E. Stanley for hosting his visit to Boston University. R.B. acknowledges the support of NSF, Div. of Materials Research.

\*Permanent address: Facultad de Farmacia, Departamento de Fisico Quimica, UCM, 28040, Madrid, Spain.

- [1] L. Gálfi and Z. Ráacz, *Phys. Rev. A* **38**, 3151 (1988).
- [2] H. Larralde, M. Araujo, S. Havlin, and H.E. Stanley, *Phys. Rev. A* **46**, 855 (1992).
- [3] E. Ben-Naim and S. Redner, *J. Phys. A* **25**, L575 (1992).
- [4] M. Araujo, S. Havlin, R. Rosenbaum, and H.E. Stanley, *Phys. Rev. Lett.* **70**, 1461 (1993).
- [5] G. T. Barkema, *Phys. Rev. E* **53**, 2017 (1996).
- [6] G. T. Dee, *Phys. Rev. Lett.* **57**, 275 (1986).
- [7] D. A. Smith, *J. Chem. Phys.* **81**, 3102 (1984).
- [8] S. Kai, S. C. Müller, and J. Ross, *J. Chem. Phys.* **76**, 1392 (1982).
- [9] M. Edward Le Van and J. Ross, *J. Phys. Chem.* **91**, 6300 (1987).
- [10] S. C. Müller, S. Kai, and J. Ross, *J. Phys. Chem.* **86**, 4294 (1982).
- [11] K. M. Pillari, V. K. Vaidyan, and M. A. Ittyachan, *Colloid Polym. Sci.* **258**, 831 (1980).
- [12] S. Shinohara, *J. Phys. Soc. Jpn.* **29**, 1073 (1970).
- [13] V. Talanquer, *J. Chem. Educ.* **71**, 58 (1994).
- [14] A. H. Sharbaugh III and A. H. Sharbaugh, Jr., *J. Chem. Educ.* **66**, 589 (1989).
- [15] R. A. Schiberi and C. Carlsen, *J. Chem. Educ.* **65**, 365 (1988).
- [16] G. Venzi and J. Ross, *J. Chem. Phys.* **77**, 1308 (1982).
- [17] A. Büki, E. Kárpáti-Smidrózki, and M. Zrínyi, *J. Chem. Phys.* **103**, 10387 (1995).
- [18] C. Wagner, *J. Colloid Sci.* **5**, 85 (1950).
- [19] B. Chopard, P. Luthi, and M. Droz, *Phys. Rev. Lett.* **72**, 1384 (1994).
- [20] D. S. Chernavskii, A. A. Polezhaev, and S. C. Müller, *Physica (Amsterdam)* **54D**, 160 (1991).